

# Turbulence in a Bose-Einstein Condensate of Dipolar Excitons in Coupled Quantum Wells

O. L. Berman,<sup>1</sup> R. Ya. Kezerashvili,<sup>1</sup> G. V. Kolmakov,<sup>1</sup> and Yu. E. Lozovik<sup>2</sup>

<sup>1</sup>*Physics Department, New York City College of Technology, CUNY, Brooklyn, NY 11201, USA*

<sup>2</sup>*Institute of Spectroscopy RAS, Troitsk, Moscow region, 142190, Russia*

The nonlinear dynamics of a Bose-Einstein condensate (BEC) of dipolar excitons trapped in an external confining potential in coupled quantum wells is analyzed. It is demonstrated that under typical experimental conditions the dipolar excitons BEC can be described by a generalized Gross-Pitaevskii equation with the local interaction between the excitons, which depends on the exciton distribution function. It is shown that, if the system is pumped at sufficiently high frequencies, a steady turbulent state can be formed.

PACS numbers: 71.35.-y, 71.35.Lk, 73.21.Fg

In the last decade, the nonlinear dynamics of the excitations in semiconductor heterostructures coupled with laser radiation attract attention because of promising potential applications in electronics and photonics, including, e.g., design of thresholdless lasers, optical computing and quantum computing [1–3]. One of the examples of the systems where the excitations demonstrate essentially quantum behavior is a Bose-Einstein condensate (BEC) of excitons in semiconductors [4–8]. The dynamics of dipolar excitons formed by spatially separated charges in coupled quantum wells (CQWs) in semiconductor heterostructures at helium temperatures attract attention due to the relatively long exciton lifetime compared to excitons in a single quantum well [6, 7]. Recently, it was predicted that dipolar excitons can form a superfluid in a two-layer graphene [9].

In this paper we focus on non-stationary dynamics in a dipolar exciton BEC in QCWs in an in-plane trapping potential. The trapping potential is essential for the condensate formation at finite temperatures and it can be formed in GaAs structures by applying inhomogeneous stress [7], static electric as well as magnetic field or laser radiation (see [8] and references therein). The dynamics of dipolar excitons is complicated due to long-range,  $\propto 1/r^3$ , interaction in the system. In the present work, we demonstrate that under certain conditions the interactions in a dipolar exciton BEC can be considered as *local interactions*. As a result, the dynamics of the BEC can be effectively described by the generalized Gross-Pitaevskii equation (GPE).

To characterize the non-stationary behavior of the dipolar exciton BEC we perform numerical simulations of the system where the resonant driving in the low- or high-frequency spectral domains is present. It was found that the dynamics of the system in these two cases are essentially different: for the low-frequency driving, the BEC spatial distribution tends to a stationary bell-like shape described well by the parabolic Thomas-Fermi profile [10] whereas for the high-frequency driving, the BEC demonstrates long-lasting, non-stationary oscillations. This os-

cillatory state is somewhat similar to the wave turbulence state observed earlier in spatially restricted nonlinear superfluid systems [11, 12].

*Local approximation for a dipolar exciton BEC.* At temperatures much lower than the BEC transition temperature, the dynamics of a dilute dipolar exciton condensate is described by the generalized two-dimensional Gross-Pitaevskii equation

$$i\hbar \frac{\partial \Psi(\mathbf{r}, t)}{\partial t} = -\frac{\hbar^2}{2m_{\text{ex}}} \Delta \Psi(\mathbf{r}, t) + V(\mathbf{r})\Psi(\mathbf{r}, t) + \Psi(\mathbf{r}, t) \times \int d^2\mathbf{r}' |\Psi(\mathbf{r}', t)|^2 U(\mathbf{r} - \mathbf{r}') + i\hbar \left( \hat{R} - \gamma \right) \Psi(\mathbf{r}, t). \quad (1)$$

In Eq. (1)  $\Psi(\mathbf{r}, t)$  is the exciton condensate wave function,  $m_{\text{ex}}$  is the exciton mass,  $V(\mathbf{r}) = \alpha r^2/2$  is an external parabolic trapping potential,  $\alpha$  is the trapping potential strength,  $U(\boldsymbol{\rho}) = e^2 D^2 / \varepsilon \rho^3$  is the pairwise exciton interaction potential,  $e$  is the electron charge,  $D$  is the inter-well distance,  $\varepsilon$  is the dielectric permittivity of the semiconductor,  $\rho = |\mathbf{r} - \mathbf{r}'|$  is the distance between the excitons, and  $\gamma = 1/2\tau_{\text{ex}}$ , where  $\tau_{\text{ex}}$  is the exciton lifetime. Below an isotropic trap is considered. However, this is not a restriction of the model and we can also consider anisotropic traps with different trapping potential strengths in  $x$  and  $y$  directions. The last term in Eq. (1) describes creation of the excitons due to the interaction with the pumping laser radiation and the exciton decay similarly to that used in earlier works [13, 14]. However, to capture the resonant pumping in a given spectral domain, we introduce a linear operator  $\hat{R}$  instead of the direct driving [13] or the homogenous, frequency-independent growth increment [14]. The  $\hat{R}$  operator is defined via its matrix elements in a functional basis that enter into the system of equations (4) given below.

The integral term in Eq. (1) diverges at small distances  $\rho$ , that corresponds to known divergence of the scattering amplitude of the dipolar excitons [4]. To regularize the integral we introduce a cutoff distance  $r_0 = (\varepsilon\mu/e^2 D^2)^{1/3}$  defined by the equation  $U(r_0) = \mu$ , where  $\mu$  is the chemical potential in the exciton system. This is equivalent

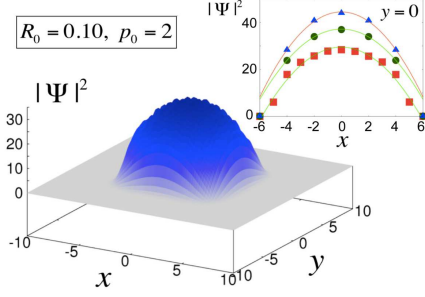


FIG. 1: Steady-state spatial distribution for the dipolar exciton BEC density in a trap for the low-frequency driving at  $R_0 = 0.1$ . Inset shows the evolution of the exciton density profile with rising the pumping rate  $R_0$ : 0.1 (■), 0.3 (●), and 0.5 (▲). The curves represent the Thomas-Fermi distribution function.

lent to the cutoff of the exciton energies at the chemical potential  $\mu$ . In this case, the function  $|\Psi(\mathbf{r}', t)|^2$  can be expanded in a Taylor series over  $\rho$  and the integral term reads  $\int_{\rho \geq r_0} d^2\mathbf{r}' |\Psi(\mathbf{r}', t)|^2 U(\rho) = g|\Psi(\mathbf{r}, t)|^2 (1 + O(r_0/a))$ , where  $g = 2\pi e^2 D^2 / \epsilon r_0$ ,  $O(r_0/a)$  denotes the terms of  $(r_0/a)$  order, and  $a \sim \Psi(\mathbf{r}, t) / |\nabla \Psi(\mathbf{r}, t)|$  is the characteristic length, at which the condensate wave function changes significantly. For the low-frequency resonant driving  $a$  coincides by the order of magnitude with the size of the exciton cloud  $d \sim 10 \mu\text{m}$  [7, 8]. Hence, the used approximation for the integral term is valid if  $r_0 \ll 10 \mu\text{m}$ . For the high-frequency driving,  $a$  can be smaller than  $d$  and is defined by the driving frequency. The estimates for the experimental conditions [7, 8] show that  $r_0/d \leq 0.04$  and therefore, the corrections  $\sim (r_0/a)$  are negligible.

Thus, under the experimental conditions [7, 8] the dynamics of the dipolar exciton BEC is described by the equation

$$i\hbar \frac{\partial \Psi(\mathbf{r}, t)}{\partial t} = -\frac{\hbar^2}{2m_{\text{ex}}} \Delta \Psi(\mathbf{r}, t) + V(\mathbf{r}) \Psi(\mathbf{r}, t) + g \Psi(\mathbf{r}, t) |\Psi(\mathbf{r}, t)|^2 + i\hbar \left( \hat{R} - \gamma \right) \Psi(\mathbf{r}, t). \quad (2)$$

Eq. (2) coincides with the “traditional” GPE, in which creation and decay of the particles are taken into account. However, in Eq. (2) the exciton interaction strength  $g$  depends on the chemical potential of the system and thus, on the density of the exciton BEC. In what follows we incorporate the equation for the chemical potential in the BEC determined for a dilute gas in a trap [10],

$$\mu = (H^{(2)} + 2H^{(4)})/N, \quad H^{(4)} = \frac{g}{2} \int d\mathbf{r} |\Psi(\mathbf{r}, t)|^4, \quad (3)$$

$$H^{(2)} = \int d\mathbf{r} \left( \frac{\hbar^2}{2m_{\text{ex}}} |\nabla \Psi(\mathbf{r}, t)|^2 + |\Psi(\mathbf{r}, t)|^2 V(\mathbf{r}) \right),$$

where  $N = (1/2) \int d\mathbf{r} |\Psi(\mathbf{r}, t)|^2$  is the total number of the excitons in the BEC, and  $H^{(2)}$  and  $H^{(4)}$  are the quadratic and fourth-order terms in the Hamiltonian of the system, respectively.

*Exciton BEC formation.* To investigate the nonlinear dynamics of a dipolar exciton BEC, we solve the system (2), (3) with the help of the spectral representation that results in the following system of equations

$$\frac{\partial A_{\mathbf{n}}}{\partial t} = -ig \sum_{\mathbf{m}, \mathbf{k}, \mathbf{l}} W_{\mathbf{n}, \mathbf{m}, \mathbf{k}, \mathbf{l}} A_{\mathbf{m}}^* A_{\mathbf{k}} A_{\mathbf{l}} + (R_{\mathbf{n}} - \gamma) A_{\mathbf{n}}, \quad (4)$$

where  $A_{\mathbf{n}}(t)$  are time-dependent spectral amplitudes,  $W_{\mathbf{n}, \mathbf{m}, \mathbf{k}, \mathbf{l}}$  is the matrix element of the interaction term  $H^{(4)}$ , and  $R_{\mathbf{n}}$  is the matrix element of the  $\hat{R}$  operator.  $A_{\mathbf{n}}(t)$  are the coefficients of the expansion of the condensate wave function,  $\Psi(\mathbf{r}, t) = \sum_{\mathbf{n}} A_{\mathbf{n}}(t) \varphi_{\mathbf{n}}(\mathbf{r})$ , where the basis functions  $\varphi_{\mathbf{n}}(\mathbf{r})$  are the eigenfunctions of the Hamiltonian for a single particle in a parabolic potential [15], and  $\mathbf{n} = (n_x, n_y)$  is the two dimensional index. The Schrödinger equation for the basis functions coincides with the linear, Hermitian part (i.e. the first two terms in the r.h.s.) of Eq. (2). This choice allows us to capture the behavior of the condensate wave function by taking into account a relatively small number of terms in the expansion for  $\Psi(\mathbf{r}, t)$  and hence, obtain a good numerical convergence. In the simulations, the length and time are expressed in the oscillatory units  $\ell_0 = (\hbar^2 / \alpha m_{\text{ex}})^{1/4} = 0.9 \mu\text{m}$ ,  $t_0 = (m_{\text{ex}} / \alpha)^{1/2} = 1.6 \text{ ns}$  calculated for the external trapping potential at  $\alpha = 50 \text{ eV/cm}^2$  and the exciton mass  $m_{\text{ex}} = 0.22m_0$ , where  $m_0$  is the free electron mass. The initial conditions were chosen in the form of quasi-equilibrium distribution  $A_{\mathbf{n}}(0) = [T / (\mu_0 + n_x + n_y + 1)]^{1/2} \exp(i\phi_{\mathbf{n}})$  with the dimensionless temperature  $T = 0.1$ , the dimensionless chemical potential  $\mu_0 = 1$ , and random phases  $\phi_{\mathbf{n}}$ . We found that the results only weakly depend on the choice of the  $T$  and  $\mu_0$  constants. We numerically integrated the system of equations (4) with the 4<sup>th</sup> order Runge-Kutta scheme on a graphical processing unit NVIDIA Tesla S2050.

We consider two cases: (a) the exciton system is pumped at low spectral modes, i.e., at frequencies comparable with the fundamental frequency in the parabolic trap,  $\omega_0 = t_0^{-1}$ ; (b) the system is pumped in the high frequency spectral domain  $\omega > \omega_0$ . It is worth noting that, in experiments the ratio of the driving frequency and the fundamental frequency of the trap may be tuned by changing both the laser pumping frequency and the trapping potential strength  $\alpha$  [7, 8].

For the low-frequency driving, we set  $R_{\mathbf{n}} = R_0$  at  $n \equiv (n_x^2 + n_y^2)^{1/2} \leq p_0$  where  $p_0$  is a given cut-off and  $R_{\mathbf{n}} = 0$  otherwise. Below, we show the results obtained for  $p_0 = 2$ . The driving was applied at  $t = 0$ . Initially, the system exhibits transient oscillations. At a later time, the oscillations were damped and the system relaxed to a stationary state, in which the spectral amplitudes  $A_{\mathbf{n}}$  tend to constant values. The time required to approach the stationary state was equal to  $t \approx 50t_0 \approx 80 \text{ ns}$  for a low pumping rate  $R_0 = 0.1$  and it decreases to  $t \approx 20t_0 \approx 32 \text{ ns}$  for a high pumping rate  $R_0 = 0.6$ . We

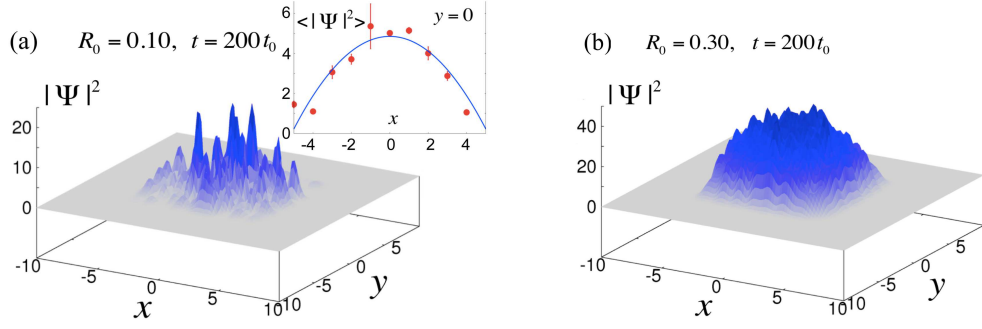


FIG. 2: The exciton density profiles at  $t = 200t_0$  for (a)  $R_0 = 0.1$  and (b)  $R_0 = 0.3$  for the high-frequency driving at  $p_1 = 4$ ,  $p_2 = 6$ . Inset on frame (a) shows the exciton density plotted at  $y = 0$  and averaged over the time period  $50t_0 < t < 200t_0$  and three independent runs (points). Curve shows the fitting by the Thomas-Fermi distribution.

also observed that the initial exciton distribution relaxed to zero if the pumping rate was less than the threshold value  $R_0 \approx 0.03$ . The presence of the finite excitation threshold is in agreement with the results of previous simulations of the polaritons dynamics [14]. Figure 1 shows the stationary non-uniform spatial distribution of the exciton BEC density at  $t = 200t_0$  for  $R_0 = 0.1$ . It is seen in Fig. 1 that an exciton “cloud” of size  $\sim 6 - 8 \ell_0$  that is,  $\sim 5 - 7 \mu\text{m}$  is formed at the center of the trap. Formation of the cloud at the center of the trap is in agreement with the observations with indirect excitons in a trap [7] and in the BECs of trapped atomic gases [10]. As is seen in the inset in Fig. 1, the spatial distribution of the exciton in the BEC can be described by the Thomas-Fermi distribution  $|\Psi(\mathbf{r})|^2 = n_0[1 - (r/d)^2]$  ( $n_0$  is the BEC density at the center of the trap and  $d$  is the effective radius of the cloud), which is used for characterization of inhomogeneous atomic BECs [10]. It is seen in Fig. 1 that the exciton density at the center of the trap gradually grows with the increase of the pumping rate.

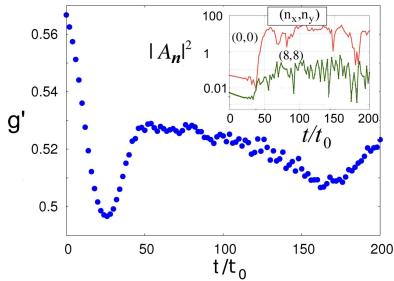


FIG. 3: Dependence of the dipolar exciton interaction strength on time for the high-frequency driving at  $p_1 = 4$ ,  $p_2 = 6$ . Inset: Time dependence of the spectral amplitudes  $|A_{\mathbf{n}}|$  at  $\mathbf{n} = (0, 0)$  (the fundamental mode) and  $(8, 8)$ .

When the system was driven in the high frequency spectral range ( $R = R_0$  at  $p_1 < n \leq p_2$ , and  $p_2 > p_1 \geq 4$ ) the BEC exhibited *persistent, non-damped oscillations*. At relatively small pumping rates,  $R_0 \sim 0.1$ , the spatial BEC profile at any given moment of time was far from the Thomas-Fermi distribution and it was represented as a series of irregular “spikes”, as seen in Fig. 2a. Never-

theless, the mean exciton BEC density distribution averaged over a long enough period of time,  $\langle |\Psi(\mathbf{r}, t)|^2 \rangle$ , was close to the Thomas-Fermi distribution, as shown in the inset in Fig. 2a. At larger pumping rates,  $R_0 \geq 0.3$ , the density oscillated around a mean parabolic profile, which was close to the Thomas-Fermi distribution (Fig. 2b). We emphasize that, unlike the case of the low frequency driving, the BEC oscillations were observed during the whole time period of the simulations  $200t_0$ , which is much longer than the time duration of the initial transient processes. Figure 3 shows the respective oscillations of the spectral harmonics,  $A_{\mathbf{n}}$ , at  $t > 50t_0$  and the variations of the dimensionless interaction strength,  $g' = gm_{\text{ex}}/\hbar^2$ , with time. A decrease of both  $A_{\mathbf{n}}$  and  $g'$  at  $t < 50t_0$  corresponds to initial relaxation after the driving was applied.

To characterize the oscillatory regime, we plot a two-dimensional amplitude distribution  $\langle |A_{\mathbf{n}}|^2 \rangle$  averaged over time and three independent runs, as a function of  $(n_x, n_y)$ , see inset in Fig. 4. It is clearly seen that, despite the system is driven at the high-frequency range (marked by dashed curves), the maximum of the spectral amplitudes (deeper color) is positioned at low spectral numbers  $n \leq 2$ . Therefore, mutual interaction between different spectral scales is present in the system. In other words, a flux of the excitations from the region, at which they are generated by an external pumping, toward the low-frequency region is formed. The resultant state is quite similar to a wave-turbulent state known for weakly nonlinear systems [16]. In those systems, nonlinear interaction of running waves resulted in formation of turbulence, which was characterized by establishing of power-like, Kolmogorov spectra of energy and particles distributions. In our case, the system is not spatially homogenous and the interacting, normal variables are present by the oscillatory modes  $A_{\mathbf{n}}$ .

To further characterize the turbulent regime, we calculate the angle-averaged distribution for the spectral amplitudes,  $N_{n_r} = \sum_{n=n_r}^{n_r+\Delta n} \langle |A_{\mathbf{n}}|^2 \rangle$ , see Fig. 4. Formation of power-like tails of the distribution  $N_{n_r} \propto n_r^m$  at frequencies below and above the characteristic driving fre-

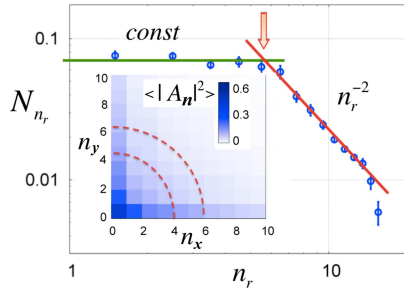


FIG. 4: Angle-averaged occupation number of the excitonic modes in the BEC,  $N_{n_r}$ , as a function of the radial number  $n_r$ , plotted in log-log scale. The data are averaged over three independent runs. The center of the pumping region is labeled by a vertical arrow,  $\Delta n = 3$ . The lines show a power-like distribution for  $N_{n_r} = \text{const} \times n_r^m$  at  $m = 0$  and  $m = -2$ . Inset shows the averaged spectral amplitude distribution  $|A_n|^2$ , the dashed curves show the boundaries of the pumping domain.

quency is clearly seen on the main part of Fig. 4, that supports our conclusion on the establishing of the turbulent regime in the dipolar exciton BEC in CQWs. The presence of two different exponents  $m = 0$  and  $m = -2$  in the low- and high-frequency domains, respectively, indicate that the fluxes of the energy and of the number of particles through the scales are simultaneously formed in the system (cf. theory for traditional GPE [16]). An essential difference between the previous considerations [16] and our results is that the effective damping in the system produced by the exciton relaxation is finite and cannot be disregarded for all modes. In effect, the fluxes of the energy and the number of particles are not completely conserved in the spectral space.

In conclusion, we demonstrate that the dynamics of the Bose-Einstein condensate of the excitons in coupled quantum wells can be described by the generalized Gross-Pitaevskii equation with the local (contact) interaction, despite a long-range dipolar exciton interaction is present. The effective interaction strength  $g$  is a function of the chemical potential of the system and therefore, should be determined self-consistently from the exciton distribution in the BEC. We show that, if the system is driven by an external pumping at low frequency modes, the spatial distribution of the excitons in a trap is described well by a parabolic density profile formerly known for dilute atomic BECs. However, if the system is driven at high frequency modes, strong time-dependent density fluctuations are excited in the BEC, and the condensate density at any given moment of time can be far from the equilibrium parabolic profile. We infer that a turbulent state is formed in the exciton BEC in this case, which is characterized by a nonlocal particle balance in the system. The latter results in formation of the power-like spectra for the exciton distribution function. The turbulent state is somewhat similar to that recently observed in superfluid  $^4\text{He}$  [11, 12] and proposed in [17] for the atomic BEC formation. The crucial difference

between all mentioned examples and the system under consideration is that in our case the interaction strength between the normal modes is a function of the occupation number of the modes. Therefore, turbulence can not be considered as “weak” and it involves more complex interactions between the modes. It is worth noting that formation of long-living nonequilibrium states was recently described for a classical system with long-range interaction [18]. The results of our consideration are useful for understanding of nonlinear phenomena in low-dimensional quantum systems including indirect excitons in CQWs [7, 8], exciton polaritons propagation [3], and a photon BEC in dye microcavities [19].

- 
- [1] A. H. MacDonald, P. M. Platzman, and G. S. Boebinger, Phys. Rev. Lett. **65**, 775 (1990); P. Littlewood, Science **316**, 989 (2007); A. A. High *et al.*, Science **321**, 229 (2008); I. Carusotto *et al.*, Phys. Rev. Lett. **103**, 033601 (2009); R. Johné *et al.*, Phys. Rev. B **81**, 125327 (2010); T. C. H. Liew and V. Savona, Phys. Rev. A **84**, 032301 (2011).
  - [2] D. W. Snoke, *Solid State Physics: Essential Concepts* (Addison-Wesley, San Francisco, 2009).
  - [3] A. Amo *et al.*, Nat. Photonics **4**, 361 (2010).
  - [4] Yu. E. Lozovik and V. I. Yudson, JETP Lett. **22**, 26 (1975);
  - [5] X. Zhu *et al.*, Phys. Rev. Lett. **74**, 1633 (1995); T. Fukuzawa, E. E. Mendez, and J. M. Hong, Phys. Rev. Lett. **64**, 3066 (1990);
  - [6] L. V. Butov *et al.*, Phys. Rev. Lett. **73**, 304 (1994); L. V. Butov *et al.*, Nature **417**, 47 (2002); L. V. Butov, A. C. Gossard, and D. S. Chemla, Nature **418**, 751 (2002).
  - [7] D. W. Snoke *et al.*, Nature **418**, 754 (2002); V. Negoita, D. W. Snoke, and K. Eberl, Phys. Rev. B **60**, 2661 (1999).
  - [8] A. A. High *et al.*, Nano Lett., Article ASAP, 2012, DOI: 10.1021/nl300983n.
  - [9] O. L. Berman, R. Ya. Kezerashvili, and K. Ziegler, Phys. Rev. B **85**, 035418 (2012).
  - [10] F. Dalfovo *et al.*, Rev. Mod. Phys. **71**, 463 (1999).
  - [11] G. V. Kolmakov *et al.*, Phys. Rev. Lett. **97**, 155301 (2006); A. N. Ganshin, V. B. Efimov, G. V. Kolmakov *et al.*, Phys. Rev. Lett. **101**, 065303 (2008);
  - [12] L. V. Abdurakhimov *et al.*, JETP Lett. **91**, 271 (2010).
  - [13] A. Amo *et al.*, Nat. Physics **5**, 805 (2009).
  - [14] J. Keeling and N. G. Berloff, Phys. Rev. Lett. **100**, 250401 (2008).
  - [15] L. D. Landau, E. M. Lifshitz, *Quantum Mechanics: Non-Relativistic Theory* (Elsevier, Oxford, 1977).
  - [16] D. Proment, S. Nazarenko, and M. Onorato, Phys. Rev. A **80**, 051603(R) (2009); A. Dyachenko and G. Falkovich, Phys. Rev. E **54**, 5095 (1996).
  - [17] Yu. Lvov, S. Nazarenko, and R. West, Physica D **184**, 333 (2003); V. E. Zakharov and S. V. Nazarenko, Physica D **201**, 203 (2005).
  - [18] F. P. C. Benetti *et al.*, Phys. Rev. Lett. **108**, 140601 (2012).
  - [19] J. Klaers *et al.*, Phys. Rev. Lett. **108**, 160403 (2012).